ACS POLYMERS Au
AN OPEN ACCESS JOURNAL OF THE AMERICAN CHEMICAL SOCIETY

pubs.acs.org/polymerau
Article

Rational Monomer Design for the Synthesis of Conjugated Polymers by Direct Heteroarylation Polymerization

Published as part of ACS Polymers Au virtual special issue "Polymer Science and Engineering in India".

Navnath R. Kakde, Himanshu Sharma, Nitin V. Dalvi, Kumar Vanka, and Asha S.K*

Cite This: ACS Polym. Au 2024, 4, 449–459
Read Online

ACCESS | Metrics & More | Article Recommendations | Supporting Information

ABSTRACT: This study focuses on the design concepts that contribute to the C−H activation in bithiophene-flanked monomers incorporating naphthalene diimide (NDI), perylene diimide (PDI), and fluorene (FLU) and their polymerization by direct heteroarylation. Density functional theory (DFT) calculations reveal distinct energy requirements for C−H bond abstraction, which is dictated by the electron-withdrawing strength of the central aromatic core flanked by bithiophene. These provide insights into the reactivity of each monomer for C−H bond activation. Proton NMR spectroscopic experimental results confirm the favorable energetic profiles predicted by DFT, with NDI- and PDI-flanked monomers exhibiting lower energy requirements than fluorene-flanked monomers. Successful polymer synthesis is demonstrated for NDI and PDI, while the fluorene-flanked monomer shows challenges due to its higher energy demands.

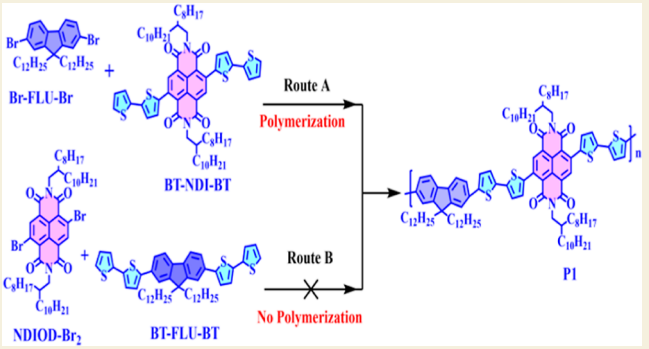

KEYWORDS: *direct heteroarylation, bithiophene-flanked monomers, naphthalene diimide, perylene diimide, fluorene, C−H activation*

INTRODUCTION

Organic conjugated polymers have attracted substantial interest of both academics and industry due to their superior electrical and optical properties.[1] Their excellent solubility enables large-scale techniques like roll-to-roll printing, facilitating the economical production of printed electronic devices.[2,3] Conjugated polymers have found applications in polymer solar cells, supercapacitors, batteries, and organic field-effect transistors.[4−8] The development of conjugated polymers relies on different coupling methods like Ziegler−Natta, Migita−Stille, Kumada, Heck, Miyaura−Suzuki, Negishi, and olefin-metathesis.[9,10] However, the synthesis of these polymers is rife with challenges, including production costs, impurities, batch variations, and scalability issues.[11] Notably, Stille cross-coupling polymerization involves organostannane monomers, and it necessitates multistep synthesis with challenging purification, generating toxic byproducts such as Me_3SnBr in stoichiometric quantities.[12,13]

Environment-friendly and atom-efficient methodologies are highly desirable for synthesizing and scaling up conjugated polymers. One promising technique that offers a convenient and feasible route for synthesizing these materials is DHAP or direct heteroarylation polymerization. The aromatic carbon−hydrogen (C−H) bonds are activated by the catalyst palladium, which facilitates the coupling, resulting in homopolymers and copolymers.[14,15] Over the last couple of years, DHAP has significantly improved, leading to highly efficient organic electronic materials with minimum environmental impact.[16,17] Despite these advancements, there are still several challenges associated with the versatility of DHAP in adapting various monomer designs.[12,18,19] New monomer design for DHAP has to mostly rely on bithiophene-flanked derivatives for producing polymers with reasonable molecular weights due to the high C−H activation energies associated with most of the arene moieties.[15,20] The different reactivities of C−H bonds have some limitations like β-defects and poor regioselectivity.[21−23] Use of such defective polymers can hamper the performance of the device.[10,24−28] Many researchers are working on improving the reactivity of α C−H bonds, specifically designing new monomers, phosphine ligands, and additives for polymerization.[12,23,24] In previous work, we synthesized a P(NDI2OD-T2) polymer in a defect-

Received: May 17, 2024
Revised: June 26, 2024
Accepted: June 26, 2024
Published: July 5, 2024

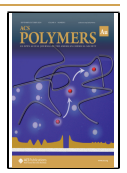

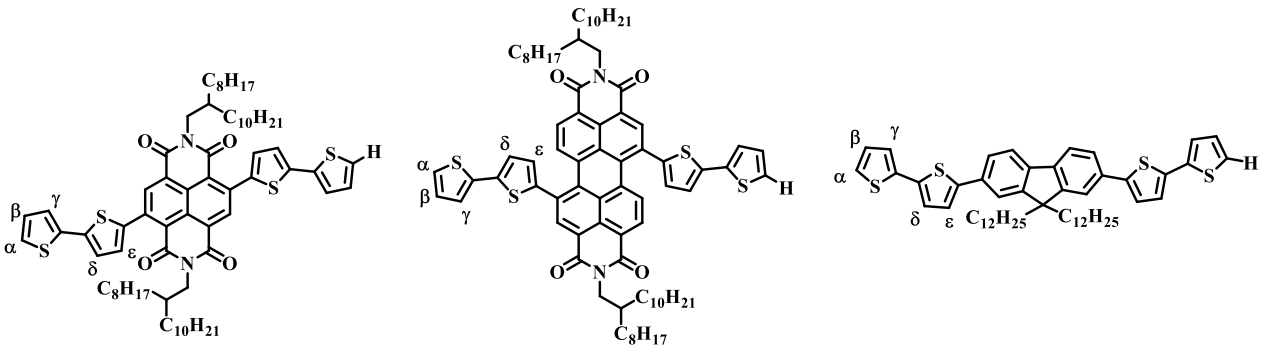

Figure 1. Chemical structure of bithiophene-flanked monomers.

free manner by the DHAP method by designing a new BT-NDI-BT monomer.[29,30]

In our continued efforts to address the challenges of DHAP and to explore the factors that contribute to or interfere with C−H activation, we have proposed schemes for DHAP with a series of bithiophene-flanked donor and acceptor moieties in this current work. The C−H reactivity of these monomers was investigated using density functional theory (DFT) and ^{1}H NMR spectroscopy. Differential scanning calorimetry (DSC), thermogravimetric analysis (TGA), and UV−visible absorption spectroscopy were made use of to characterize the polymers.

EXPERIMENTAL SECTION

Materials

1,4,5,8-Naphthalenetetracarboxylic dianhydride (NTCDA), 3,4,9,10-perylenetetracarboxylic dianhydride (PTCDA), 2-octyl dodecanol, triphenylphosphine, potassium phthalimide, molecular bromine (Br_2), hydrazine hydrate, oleum, and iodine (I_2) were purchased from TCI and used without further purification. Bithiophene, pivalic acid, palladium acetate ($Pd(OAc)_2$), tris(4-methoxyphenyl)phosphine, CS_2CO_3, trimethyltin chloride, *t*-butyl toluene, toluene, 1,1,2,2-tetrachloroethane-d_2 (TCE-d_2), and chloroform-*d* ($CDCl_3$) were purchased from Sigma-Aldrich and used without further purification. *tert*-Butyl toluene, 1,2,4-trichlorobenzene (TCB), toluene, and chlorobenzene were also purchased from Sigma-Aldrich and used after drying. Sodium thiosulfate (Na_2SO_4), ammonium chloride (NH_4Cl), and magnesium sulfate ($MgSO_4$) were purchased from Loba Chemie Pvt Ltd. Acetone, hexane, methanol (MeOH), chloroform ($CHCl_3$), dichloromethane (DCM), tetrahydrofuran (THF), and ethyl acetate were purchased from Merck.

Measurements and Methods

The structural characterization of small molecules and monomers was conducted by recording ^{1}H and ^{13}C NMR spectra at 25 °C on Bruker-AVENS 200 and 400 MHz NMR instruments. Deuterated chloroform ($CDCl_3$) was used as the solvent, with a trace amount of TMS serving as an internal reference. The chemical shifts of the NMR peaks are reported in ppm. The mass of the monomer was determined using an Applied Biosystem 4800 PLUS matrix-assisted laser desorption/ionization (MALDI) TOF/TOF analyzer. For the polymer structural characterization, ^{1}H NMR spectroscopy was performed at 25 °C using deuterated 1,1,2,2-tetrachloroethane (TCE-d_2) as the solvent on a Bruker-AVENS 400 MHz NMR instrument. The number-average (M_n) and weight-average (M_w) molecular weights were determined through size exclusion chromatography (SEC) using a high-temperature Agilent PL-GPC 220 system equipped with an RI detector. The column consisted of Agilent PLgel 10 μm MIXED-B, 300 × 7.5 mm (part no. PL1110-6100), columns. The flow rate was fixed at 1 mL/min using TCB as the eluent, and the temperature was set at 140 °C. To prepare the samples, 2 mg of the polymer was dissolved in 2 mL of TCB in a chromatography vial and heated at 100 °C for 1 h to ensure complete dissolution. Subsequently, the samples were filtered by using a 0.45 μm PVDF filter. Polystyrene narrow standards Easi-Vials PS-M from Varian Polymer Laboratories dissolved in TCB was employed for calibration purposes. TGA was carried out using a PerkinElmer STA (Simultaneous Thermal Analyzer) 6000 thermogravimetric analyzer. The heating rate was set at 10 °C/min, and the samples were heated from 40 to 900 °C under a nitrogen atmosphere. DSC was performed using a TA Discover 250 s-generation instrument. The samples were subjected to a heating rate of 10 °C/min from −10 to 330 °C under a nitrogen atmosphere. The absorption spectra were recorded using a double-beam PerkinElmer lambda-35 UV/vis spectrometer with deuterium and tungsten lamps as the source.

RESULTS AND DISCUSSION

Monomer Design

According to the findings of Mario Leclerc and co-workers, achieving selectivity in C−H bond activation at the α-position is influenced by many factors.[14,15,18,19] Their research demonstrated that the selective polymerization of unprotected thiophene units could be effectively achieved by DHAP when paired with the correct catalyst, additive, and ligand. It is worth noting that the utilization of P(o-NMe_2Ph)$_3$ with a Herrmann−Beller catalyst and a bulky acidic additive in dioxane solvent resulted in well-defined thiophene−thiophene couplings.[31] Additionally, Mario Leclerc and his research team conducted a comprehensive study involving DFT calculations on a range of halogenated and nonhalogenated thiophene-based comonomers with both electron-rich and electron-deficient properties. The calculations revealed that bromine atoms reduce the energy required for activating adjacent C−H bonds, which can lead to undesired β-defects in certain brominated aromatic units.[32,33] The inclusion of thiophene-flanked monomers is crucial for the production of organic conjugated polymers. This is attributed to the enhanced reactivity of thiophene in C−C coupling reactions, which facilitates the integration of various donor and acceptor molecules within the conjugated system.[29] In this study, we have designed bithiophene-flanked monomers containing naphthalene diimide (NDI), perylene diimide (PDI), and fluorene. The details of the synthetic procedures and structural characterizations for $NDIODBr_2$, $PDIODBr_2$, BT-NDI-BT, BT-PDI-BT, and BT-FLU-BT are provided in the Supporting Information section (S1−S11) and Figures S1−S20. Figure 1 shows the chemical structures of the three different bithiophene-flanked monomers. Distinct energy requirements are predicted for the abstraction of C−H bonds from BT-NDI-BT, BT-PDI-BT, and BT-FLU-BT for facilitating DHAP

https://doi.org/10.1021/acspolymersau.4c00050
ACS Polym. Au 2024, 4, 449−459

polymerization. The calculated energy values determined through DFT studies provide insights into the reactivity and stability of each monomer during C−H bond abstraction.

Quantum chemical calculations were carried out employing DFT, which utilized hybrid functionals, particularly B3LYP, to guarantee the precision of the analyses. Detailed methodology information can be found in the Supporting Information. Examination of the structure of the monomers such as BT-NDI-BT, BT-FLU-BT, and BT-PDI-BT involves the abstraction of α-protons from the bithiophene unit in each monomer. The initial exploration focused on measuring the energy required to abstract the α-protons from the bithiophene moiety of each monomer. To allow for a direct comparison of the energies required for α-proton abstraction among different monomers, pristine bithiophene was defined as the reference. Specifically, the energy needed for α-proton abstraction from bithiophene was established at 0.0 kcal/mol, and the energy for β-proton abstraction was 10.0 kcal/mol. This reference framework facilitated the calculation of relative abstraction energies for all monomers compared to bithiophene.

The DFT calculations revealed significant differences in energy when abstracting α-protons from various bithiophene-flanked monomers. In the case of the BT-NDI-BT monomer, the energy required for α-proton abstraction was notably lower, measuring 8.1 kcal/mol less than that of the pristine bithiophene. Table 1 provides the details of the free energy required for α- and β-proton abstraction from their respective monomers. On the other hand, for BT-FLU-BT, α-proton abstraction necessitated a slightly higher energy, registering 0.4 kcal/mol above that of the reference bithiophene. These computational results strongly support the notion that α-proton abstraction from the BT-NDI-BT monomer is more favored energetically compared to that from the BT-FLU-BT monomer, presenting an advantage of 8.5 kcal/mol using the BT-NDI-BT monomer.

Table 1. Free Energy (ΔG_{sol}) Required for α- and β-Proton Abstraction from Their Respective Monomers[a]

sr. no	monomers	$\Delta G_{\alpha\text{-proton}}$	$\Delta G_{\beta\text{-proton}}$	$\Delta\Delta G_{(\beta\text{-proton-}\alpha\text{-proton})}$
1	bithiophene	0.0	10.0	10.0
2	BT-FLU-BT	0.4	10.1	9.7
3	BT-NDI-BT	−8.1	2.4	10.5
4	BT-PDI-BT	−7.2	3.8	12.0

[a]The energy values are expressed in kcal/mol. Level of theory: B3LYP-D3/def2-TZVP.

The observed differences in energy levels can be attributed to charge delocalization, which helps to stabilize the generated conjugate base after the removal of a proton. It is worth noting that the analysis of natural charges, carried out using natural bond orbital (NBO) calculations, indicated a more significant delocalization of negative charge on the α-carbon (C_α) of the conjugated base in the bithiophene unit of BT-NDI-BT. This is supported by the lower charge observed in comparison to BT-FLU-BT and the reference bithiophene. The specific NBO charge values for the α and β carbons of all monomers can be found in Table 2. The findings are supported by the analysis of frontier molecular orbitals (FMOs), which confirms the relative softness (reactivity) of monomer BT-NDI-BT when compared to those of BT-FLU-BT and bithiophene. Figure 2 displays the HOMO−LUMO energy profiles for bithiophene, BT-PDI-BT, BT-FLU-BT, and BT-NDI-BT monomers. BT-NDI-BT exhibited a narrower HOMO−LUMO energy gap (ΔE_{H-L}) of 2.0 eV, in contrast to 2.9 eV for BT-FLU-BT and 4.0 eV for the reference bithiophene. These results collectively offer valuable insights into the reactivity profiles of the designed monomers.

The DFT calculations also show that the energy needed for α-proton abstraction from the bithiophene unit of monomer BT-PDI-BT is 7.2 kcal/mol lower than that of the reference bithiophene and 6.08 kcal/mol lower than that of the BT-FLU-BT monomer. Moreover, the reduced HOMO−LUMO gap of the BT-PDI-BT monomer, which is measured at 1.8 eV, indicates its increased reactivity compared to that of the BT-FLU-BT monomer. Comprehensive computational analyses have provided insights into the lower energy requirements for α-proton abstraction from BT-NDI-BT and BT-PDI-BT monomers in comparison to those from the BT-FLU-BT and reference bithiophene monomers. The conjugate base of BT-NDI-BT and BT-PDI-BT monomers exhibited improved stability when compared to the BT-FLU-BT monomer.[29] This can be attributed to the strong electron-withdrawing properties of NDI and PDI relative to the fluorene unit.

Experimental support for the observations from the DFT studies could be obtained from ^{1}H NMR experiments conducted in TCE-d_2 (deuterated 1,1,2,2-tetrachloroethane). A deshielded (downfield) proton shift in the NMR spectra indicates a higher electron-withdrawing nature. Figure 3 depicts the expanded region in the proton NMR spectra of the three bithiophene-flanked monomers. The ^{1}H NMR spectra confirmed that NDI and PDI moieties exhibited a higher electron-withdrawing nature, as evidenced by more pronounced downfield chemical shifts compared with the bithiophene-flanked fluorene moieties.

Analysis of the proton shift involved in the C−H activation on the bithiophene ring is crucial as protons play a key role in the direct heteroarylation process. Through detailed NMR spectroscopic investigations, the chemical shift of various protons on the bithiophene unit was determined and confirmed. 2D heteronuclear multibond correlation (HMBC) spectroscopy was utilized to investigate the connectivity and sequence of protons and carbons on the bithiophene unit. The

Table 2. NBO Charge on α and β Carbons of All Monomers[a]

monomer	neutral case		α-H abstraction (conjugated base)		β-H abstraction	
	C_α	C_β	C_α	C_β	C_α	C_β
bithiophene	−0.417	−0.251	−0.548	−0.397	−0.464	−0.426
BT-Flu-BT	−0.411	−0.252	−0.521	−0.384	−0.454	−0.418
BT-NDI-BT	−0.40	−0.250	−0.474	−0.354	−0.449	−0.317
BT-PDI-BT	−0.183	−0.150	−0.473	−0.353	−0.457	−0.290

[a]Level of theory: B3LYP-D3/def2-TZVP.

https://doi.org/10.1021/acspolymersau.4c00050
ACS Polym. Au 2024, 4, 449−459

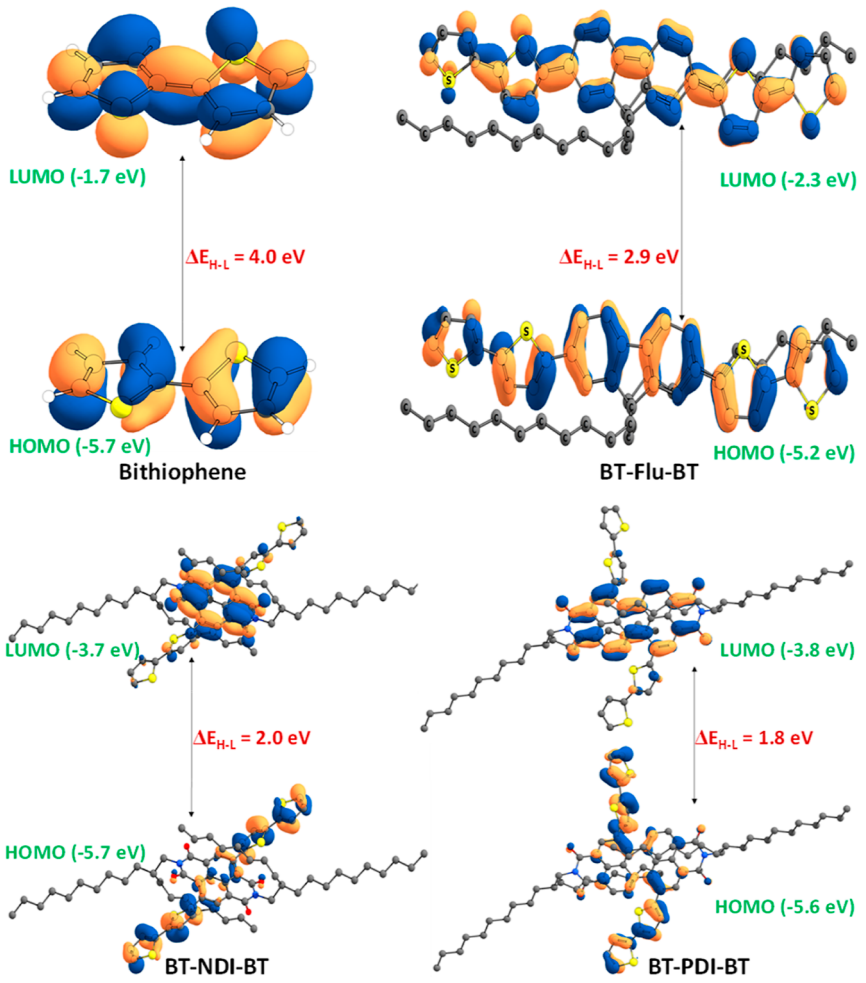

Figure 2. HOMO−LUMO energy profiles for bithiophene (reference), BT-FLU-BT, BT-NDI-BT, and BT-PDI-BT. All the hydrogen atoms are omitted for the purpose of clarity. The isosurface value is 0.03. Level of theory: B3LYP-D3/def2-TZVP.

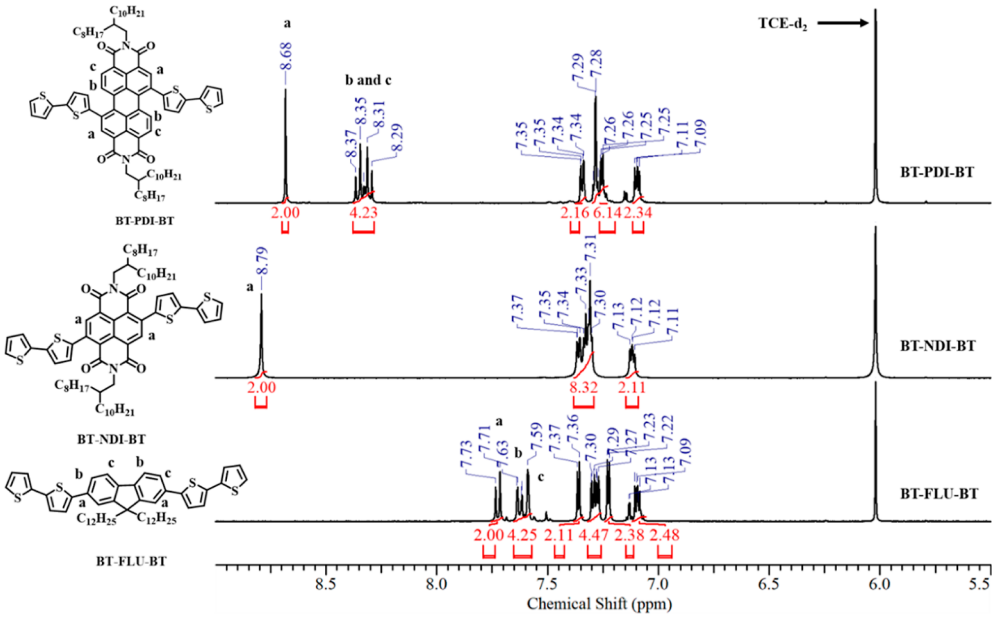

Figure 3. Aromatic region (zoomed) in the ^{1}H NMR spectra for BT-FLU-BT, BT-NDI-BT, and BT-PDI-BT monomers, recorded in 1,1,2,2-tetrachloroethane-d_2 (TCE-d_2) at 25 °C.

https://doi.org/10.1021/acspolymersau.4c00050
ACS Polym. Au 2024, 4, 449−459

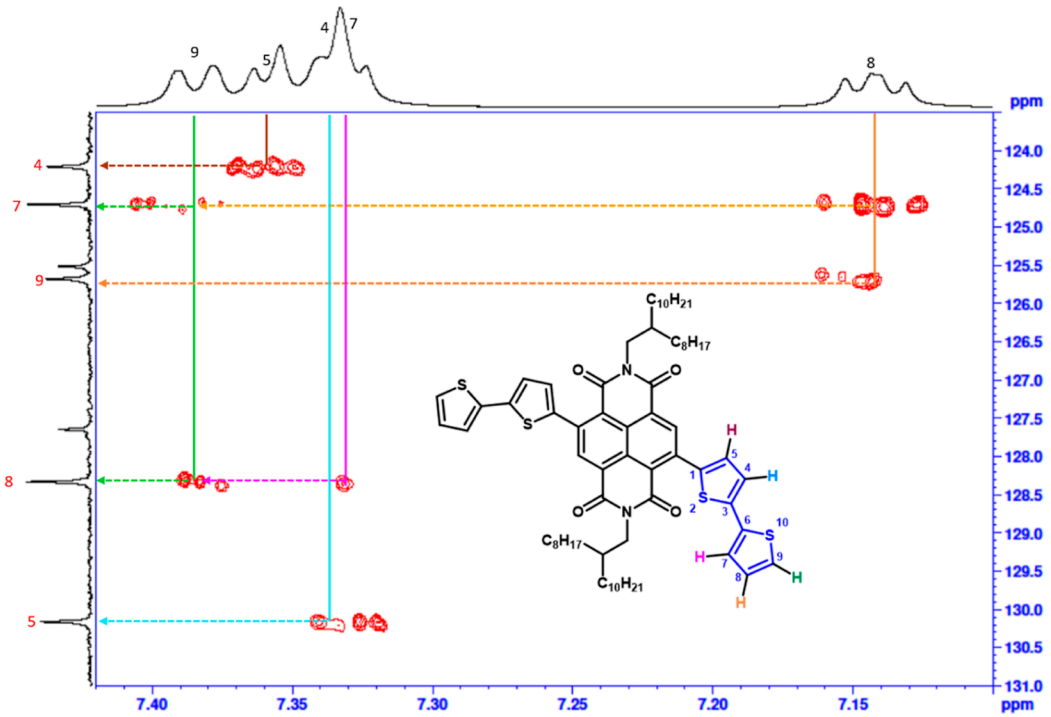

Figure 4. HMBC spectrum for the BT-NDI-BT monomer, and the dotted line shows contour correlations.

2D HMBC spectrum for the BT-NDI-BT monomer as shown in Figure 4 highlights the contour correlations observed.

For instance, the correlation of carbon C9−C8−C7 for the terminal thiophene ring was confirmed through the contour of H-9 (7.38 ppm) [labeled as carbon-9 (green proton) in structure and also peak marked as 9 on 2D projections] with C7 (124.7 ppm) (carbon labeled 7) and C8 (128.3 ppm). Correlation could also be established for H-8 (7.14 ppm) with C9 (125.7 ppm) and C7 (124.7 ppm). Similarly, a contour for H-7 (7.33 ppm) established a correlation with C8 (128.3 ppm) and C9 (125.7 ppm). Hence, these contours confirm the correlation of carbon C9−C8−C7 for the terminal thiophene ring. Moreover, correlations between H-4 and H-5 with their respective carbons further support the peak assignment to the thiophene ring adjacent to the NDI moiety in the structure.[34]

Further evidence was collected through the execution of a nuclear Overhauser effect (1D-NOE) NMR experiment. The 1D-NOE spectrum for BT-NDI-BT is displayed in Figure S21, with the NDI ring proton at 8.81 ppm being irradiated, resulting in a NOE effect at 7.35 ppm (H-5 proton). This definitely confirmed that the H-5 proton was part of the ring adjacent to the NDI moiety of structure.[35] The identification of the protons of the inner and outer thiophene rings of the bithiophene was facilitated by through-bond proton−proton correlation (2D correlation spectroscopy; COSY) and heteronuclear single quantum coherence spectroscopy (HSQC) experiments, which correlated the chemical shift of protons to the 13C chemical shift of their directly attached carbons. The specific thiophene proton values (δ ppm) of the BT-NDI-BT monomer are listed in Table 3, and the NMR spectra are included in the Supporting Information (2D COSY, HSQC) Figures S22−S24. The detailed NMR analysis confirmed that the inner thiophene ring containing H-5,4 was adjacent to the NDI moiety, while the outer thiophene ring containing H-9,8,7 was located at the terminal position. These investigations also revealed that H-9 at 7.38 ppm was the most deshielded proton of the thiophene in the BT-NDI-BT monomer.

Table 3. ^{1}H NMR Chemical Shift Values (δppm) for the Thiophene Proton of BT-NDI-BT, BT-PDI-BT, and BT-FLU-BT Monomers

monomers	bithiophene protons in δ ppm				
	9 (α)	8 (β)	7 (γ)	5 (ε)	4 (δ)
BT-NDI-BT	**7.38**	7.14	7.33	7.35	7.33
BT-PDI-BT	**7.36**	7.12	7.27	7.30	7.30
BT-FLU-BT	7.32	7.12	7.3	**7.38**	7.25

Similar NMR experiments were conducted on BT-PDI-BT and BT-FLU-BT monomers. The 2D HMBC spectra for BT-PDI-BT and BT-FLU-BT are given in Figures 5 and 6, respectively. In the case of BT-PDI-BT, a correlation was observed for H-9 at 7.36 ppm, which exhibited contours with C7 (124.7 ppm) and C8 (128.3 ppm), confirming their identification as part of the terminal thiophene ring. Additionally, H-4 at 7.30 ppm and C5 (128.6 ppm) displayed contours with C5 and C4 (125.3 ppm), respectively, confirming their association with the thiophene ring adjacent to the PDI moiety. Furthermore, the most deshielded proton for the BT-PDI-BT monomer was H9 at 7.36 ppm. The spectra (2D COSY, HSQC) are provided in Figures S25−S27 of the Supporting Information, and the values are tabulated in Table 3.

The 2D HMBC spectrum (Figure 6) displayed contour correlation for H-5 (7.38 ppm) with C4 (124.9 ppm) and H-4 (7.25 ppm) with C5 (123.8 ppm), confirming the assignment to the thiophene ring adjacent to the FLU moiety in the structure of the BT-FLU-BT monomer. Similarly, there was contour correlation among H-9 (7.32 ppm) with C7 (123.9 ppm) and C8 (128.2 ppm), H-8 (7.12 ppm) with C7 (123.9 ppm) and C9 (124.7 ppm), and H-7 (7.30 ppm) with C9 (124.7 ppm) and C8 (128.22 ppm). The cross contours

https://doi.org/10.1021/acspolymersau.4c00050
ACS Polym. Au 2024, 4, 449−459

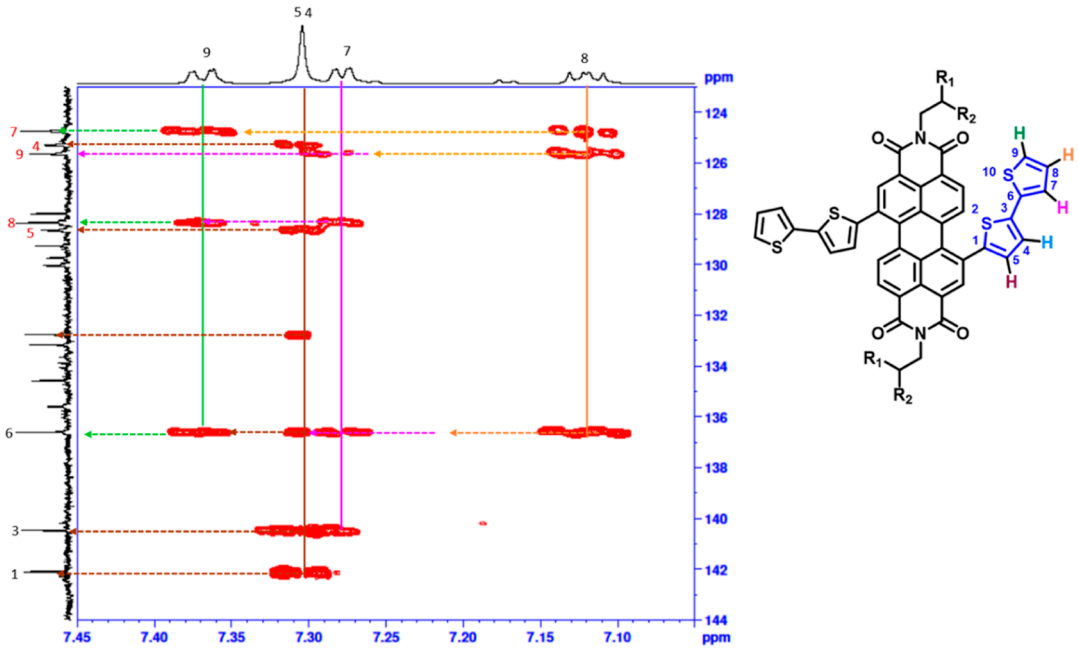

Figure 5. HMBC spectrum for the BT-PDI-BT monomer, and the dotted line shows contour correlations.

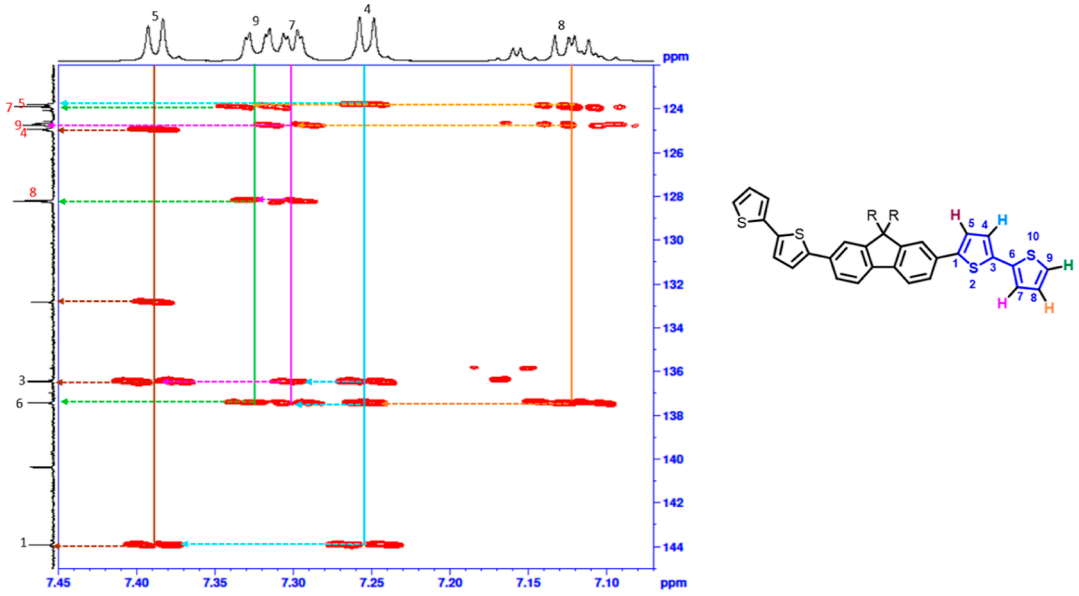

Figure 6. BT-FLU-BT part of the HMBC spectrum, and the dotted line shows contour correlations.

between H9−H8−H7 indicate the terminal thiophene ring. Notably, in the BT-FLU-BT monomer, H-5 (7.38 ppm) was the most deshielded proton of the bithiophene ring. This is in contrast to the observation for the other two monomers, where H-9 was the most deshielded proton. The detailed thiophene proton value (δ ppm) of the BT-FLU-BT monomer is tabulated in Table 3, and detailed spectra are provided in Supporting Information (2D COSY, HSQC) Figures S28−S30. This observation aligns with the DFT study, which showed that lower energy was required for the C−H bond abstraction in the case of BT-NDI-BT and BT-PDI-BT compared to that for BT-FLU-BT.

POLYMER SYNTHESIS AND CHARACTERIZATIONS

Scheme 1 shows the synthetic protocol adopted to develop copolymers of bithiophene-flanked naphthalene and perylene with fluorene as the comonomer. The importance of choosing the appropriate monomer to bear the halogen (bromine) atom in a DHAP process has been very well established in the literature.[29] Almost of equal importance is the nature of the aromatic comonomer that should be chosen as the thiophene-flanked unit. Scheme 1 illustrates that the identical polymer repeat unit can be achieved through the utilization of either Route A or Route B. Both bis bromo fluorene and bis bromo-NDI have already been demonstrated for direct heteroarylation polymerization.[24,36] Route A involved the reaction of 1 equiv of bis bromo fluorene monomer with 1 equiv of bithiophene-flanked naphthalene (BT-NDI-BT) or perylene bisimide (BT-

https://doi.org/10.1021/acspolymersau.4c00050
ACS Polym. Au 2024, 4, 449−459

Scheme 1. Synthesis of P1 and P2 Polymers Using Different Monomers by the DHAP Method

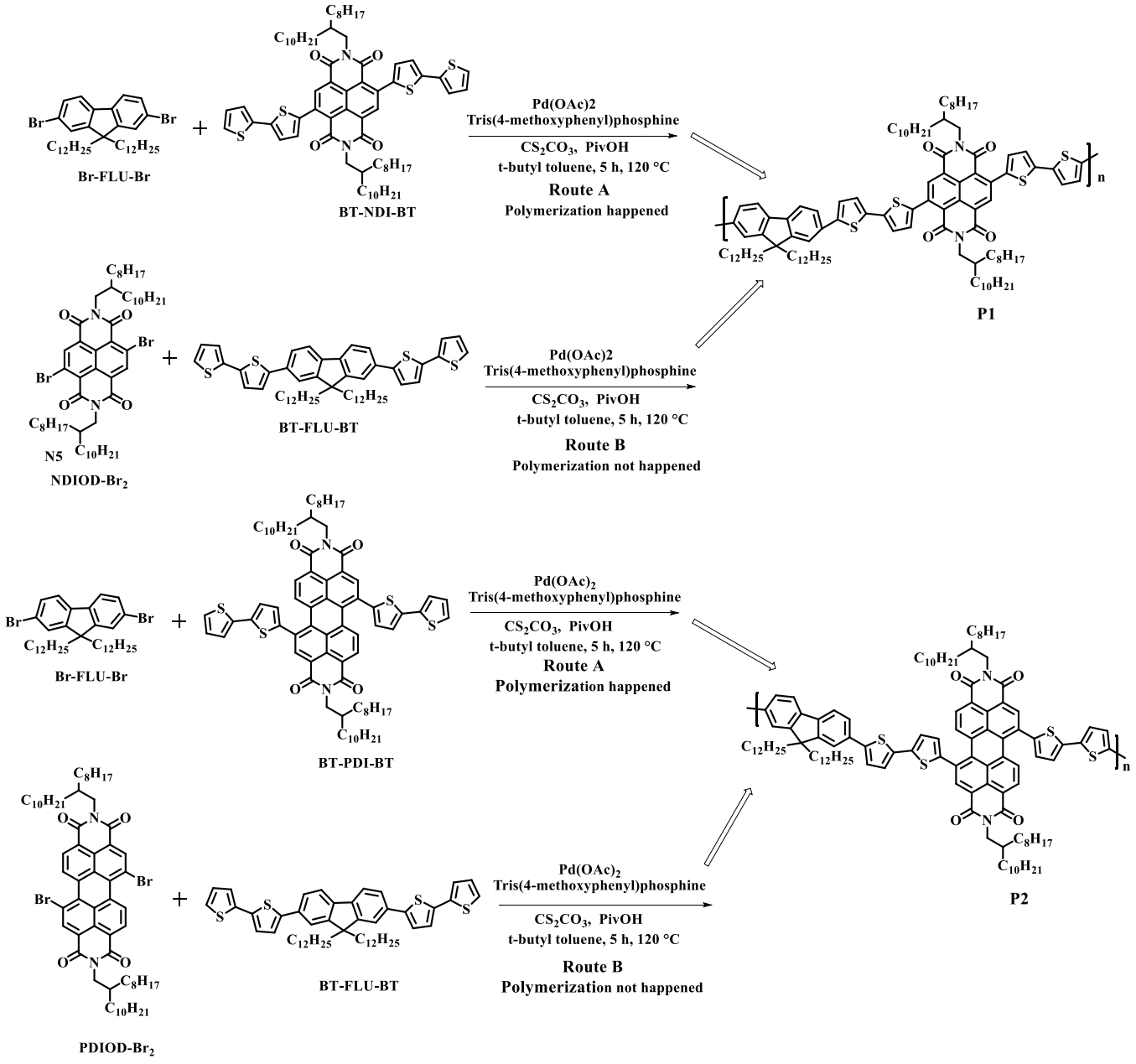

PDI-BT) as comonomer in the presence of the catalyst, ligand, additive, and solvent for 5 h at 120 °C to yield copolymers named P1 and P2, respectively. Route B was designed to arrive at the same polymer structure (P1/P2) by the reaction of bis bromo rylene bisimide with bithiophene-flanked fluorene comonomer under identical conditions. Following route A, polymer P1 could be synthesized having molecular weight M_n/M_w = 36.6/64.4 kDa and yield of 96%. The perylene-substituted copolymer P2 was also synthesized by route A, resulting in a M_n/M_w of 10.5/26.9 kDa molar mass of the polymer. The details of synthesis of P1 and P2 polymers are provided in S12 and S13. However, route B did not result in polymerization with both bisbrominated NDI or PDI monomer, highlighting the importance of choice of electron-rich or electron-poor aromatic core as the thiophene-flanked comonomer unit in a DHAP synthetic scheme. The reaction conditions and results are summarized in Table 4. As detailed in the DFT section, higher energy was required for activating the C−H bond extraction for monomer BT-FLU-BT compared to monomers BT-PDI-BT and BT-NDI-BT. This disparity in the energy demands was reflected in the polymer molecular weight and yields.

Table 4. Optimized Table for the Synthesis of P1 and P2 Polymers[c]

polymers	route[a]	M_n (kg mol^{-1})	M_w (kg mol^{-1})	$Đ$	yield[b]
P1	route A	36.6	64.4	1.8	96
	route B	no polymer formed			
P2	route A	10.5	26.9	2.6	76
	route B	no polymer formed			

[a]Synthesis of P1 and P2 by different routes. [b]Yield of polymer calculated after Soxhlet purification. [c]The temperature was maintained at 120 °C and polymerization time was kept at 5 h. The catalyst ($Pd(OAc)_2$) concentration was maintained at 4 mol %.

https://doi.org/10.1021/acspolymersau.4c00050
ACS Polym. Au 2024, 4, 449−459

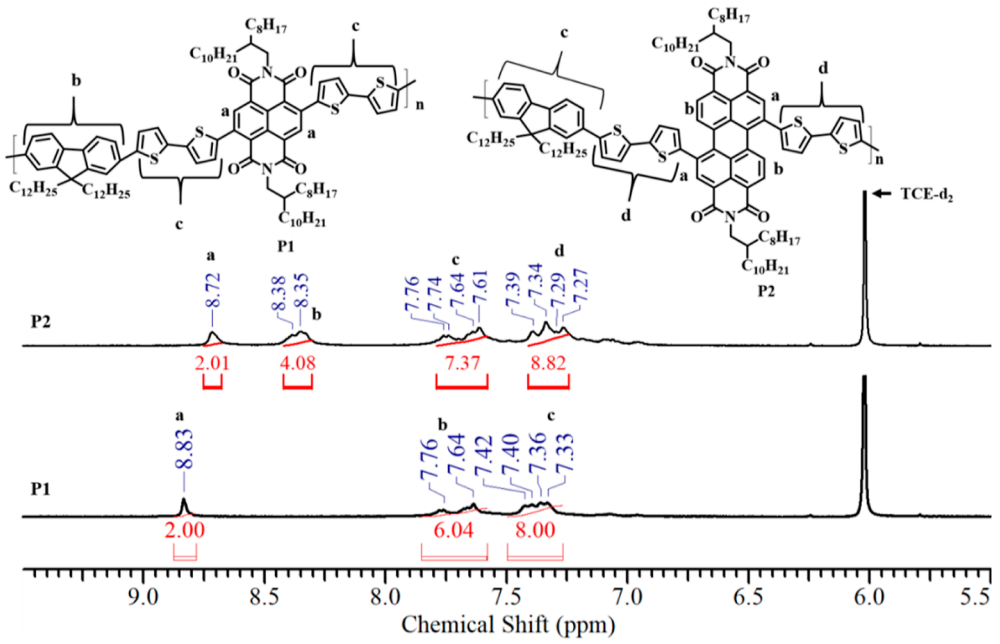

Figure 7. Aromatic region (zoomed) in the ^{1}H NMR spectra for the two polymers recorded in 1,1,2,2-tetrachloroethane (TCE-d_2) at 25 °C.

1H NMR spectroscopy confirmed the chemical structure of the polymers. Figure 7 shows the aromatic region in the 1H NMR spectra of the polymers along with their labeled structures. The complete spectra are available in Figure S31. For polymer P1, the two aromatic protons of NDI (labeled a) appeared at a chemical shift (δ) of 8.83. The chemical shift values in the range of 7.76 to 7.64 (labeled b) corresponded to the fluorene aromatic protons. The aromatic protons in the bithiophene region (labeled c) were observed between 7.42 and 7.33 ppm. In polymer P2, the peaks at 8.72 ppm (labeled a) and peaks in the range from 8.38 to 8.35 ppm indicated the incorporation of PDI. The ^{1}H NMR spectra for both polymers showed proton ratios consistent with their expected chemical structure.

Table 5 summarizes the photophysical properties of the copolymers P1 and P2, and their UV−vis absorption spectra

Table 5. Photophysical and Thermal Characterization Data for the Polymers

polymers	UV−visible absorption[a]		$T_{d(10\%)}$ (°C)[b]	T_m (°C)[c]	ΔH_m (J/g)[d]
	$\pi-\pi^*$ (nm)	ICT (nm)			
P1	409	634	441		
P2	415	636	426		

[a]UV−visible absorption spectra recorded in $CHCl_3$. [b]Determined by thermal gravimetric analysis. [c]Determined by DSC. [d]Determined by DSC.

are given in Figure 8. The polymers exhibited two absorption bands. The first absorption peak assigned to the $\pi-\pi^*$ transitions of the polymer backbone was observed at 409 and 415 nm for P1 and P2, respectively. A second low-energy absorbance peak corresponding to intramolecular charge transfer (ICT) band, which is an indication of the electronic interaction between the electron-poor and electron-rich units, was observed at 634 and 636 nm for P1 and P2, respectively. The higher intensity for the ICT band in P1 pointed to

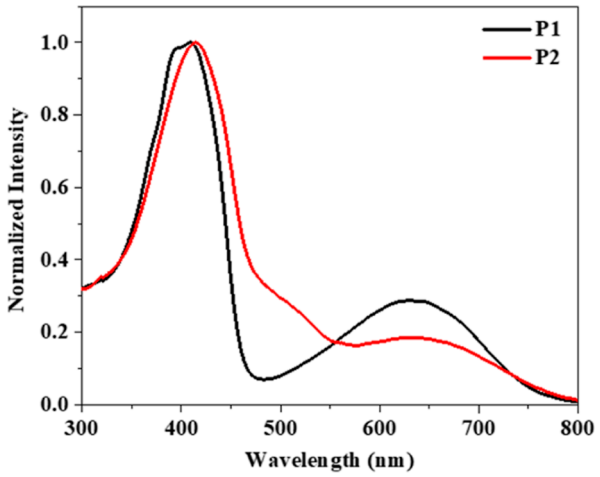

Figure 8. Absorption spectra of polymers recorded in chloroform.

enhanced interaction between the NDI and fluorine units.[37,38] The decreased intensity of the charge transfer band in P2 can be attributed to reduced planarity of the polymer backbone arising from the heightened steric hindrance caused by the larger PDI unit.[39]

The polymers were found to be highly thermally stable with $T_{d(10\%)}$ of 441 and 426 °C for P1 and P2, respectively, as determined by TGA (Figure 9). DSC analysis did not show any clear glass transition temperature, indicating the amorphous nature of the polymers. The copolymer of NDI and bithiophene (N2200) is a semicrystalline polymer.[5] The inclusion of the fluorene unit disrupts the $\pi-\pi$ stacking of the naphthalene aromatic core, resulting in an amorphous random copolymer.[40]

CONCLUSIONS

We have successfully designed and synthesized bithiophene-flanked monomers incorporating NDI, PDI, and fluorene and demonstrated the feasibility of their copolymerization by the direct heteroarylation route. DFT calculations provided

https://doi.org/10.1021/acspolymersau.4c00050
ACS Polym. Au 2024, 4, 449−459

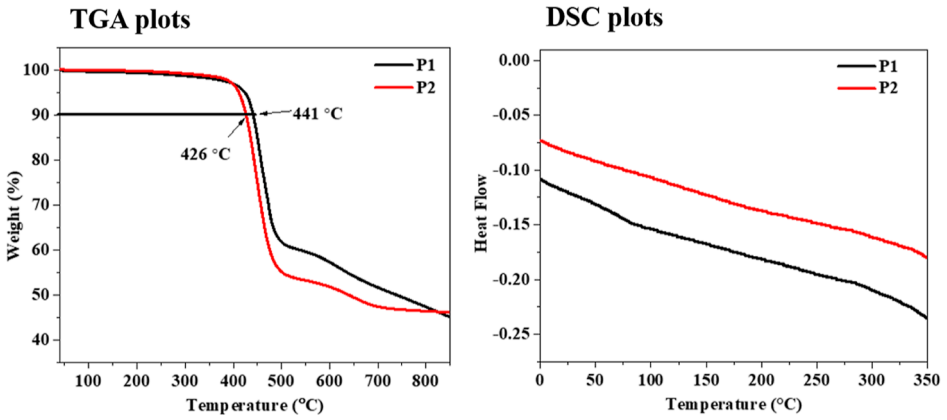

Figure 9. Thermogravimetry and DSC plots for polymers.

valuable insight into the distinct energy requirement for C−H bond abstraction in polymerization, revealing the reactivity and stability of each monomer. Proton NMR experimental analysis confirmed the favorable energetic profiles predicated by DFT, with NDI- and PDI-flanked monomers. The DFT calculations, ^{1}H NMR spectroscopy, and various characterizations provided comprehensive insights into the structural, optical, and thermal properties of the synthesized polymers. Integrating computational prediction with experimental validations has contributed to the development of a new monomer for DHAP and the synthesis of copolymers with tailored properties. This work advances the understanding of conjugated polymer design, offering a promising approach to the development of efficient and cost-effective materials for different applications.

■ ASSOCIATED CONTENT

Supporting Information

The Supporting Information is available free of charge at https://pubs.acs.org/doi/10.1021/acspolymersau.4c00050.

Experimental procedure, synthetic scheme and procedure of $NDIODBr_2$ and $PDIODBr_2$; ^{1}H NMR, ^{13}C, and MALDI-TOF spectra; synthetic scheme and procedure of BT-NDI-BT, BT-PDI-BT and BT-FLU-BT; detailed study of BT-NDI-BT, BT-PDI-BT, and BT-FLU-BT monomers by ^{1}H NMR spectroscopy (1D-NOE experiment, DEPT135 and ^{13}C, COSY, and HSQC); polymer synthesis; ^{1}H NMR spectra of polymers (P1 and P2); SEC graphs of polymers; and computational details with optimized XYZ coordinates for BT-NDI-BT, BT-PDI-BT, and BT-FLU-BT monomers (PDF)

■ AUTHOR INFORMATION

Corresponding Author

Asha S.K − *Polymer Science and Engineering Division, CSIR-National Chemical Laboratory, Pune 411008, India; Academy of Scientific and Innovative Research, Ghaziabad 201002 Uttar Pradesh, India;* orcid.org/0000-0002-3999-4810; Email: sk.asha@ncl.res.in

Authors

Navnath R. Kakde − *Polymer Science and Engineering Division, CSIR-National Chemical Laboratory, Pune 411008, India; Academy of Scientific and Innovative Research, Ghaziabad 201002 Uttar Pradesh, India;* orcid.org/0000-0002-2233-5691

Himanshu Sharma − *Physical and Materials Chemistry Division, CSIR-National Chemical Laboratory, Pune 411008 Maharashtra, India; Academy of Scientific and Innovative Research, Ghaziabad 201002 Uttar Pradesh, India*

Nitin V. Dalvi − *Polymer Science and Engineering Division, CSIR-National Chemical Laboratory, Pune 411008, India; Academy of Scientific and Innovative Research, Ghaziabad 201002 Uttar Pradesh, India; Department of Chemistry, Indian Institute of Science Education and Research (IISER Pune), Pune 411008 Maharashtra, India*

Kumar Vanka − *Physical and Materials Chemistry Division, CSIR-National Chemical Laboratory, Pune 411008 Maharashtra, India; Academy of Scientific and Innovative Research, Ghaziabad 201002 Uttar Pradesh, India;* orcid.org/0000-0001-7301-7573

Complete contact information is available at: https://pubs.acs.org/10.1021/acspolymersau.4c00050

Author Contributions

N.R.K.: development of methodology, conceptualization, formal analysis, writing—original draft, investigation, and visualization. H.S.: DFT studies, formal analysis, and writing. N.V.D.: ^{1}H NMR study, formal analysis, and writing. K.V.: DFT studies and writing—review editing. A.S.K.: conceptualization, formal analysis, investigation, writing—original draft, and writing—review editing.

Notes

The authors declare no competing financial interest.

■ ACKNOWLEDGMENTS

This work has been financially supported by SERB project SPF/2021/000135 and the Facility Creation Project (FCP; no. 34/FCP/NCL/2019-RPPBDD) supported by the Council of Scientific and Industrial Research, Project Planning & Business Development Directorate, New Delhi. Navnath R. Kakde thanks CSIR for the senior research fellowship (SRF). The authors would like to thank Professor M Jayakannan, IISER Pune, for the fruitful discussions throughout the execution of this project.

■ REFERENCES

(1) Ueda, K.; Tanaka, K.; Chujo, Y. Optical, Electrical and Thermal Properties of Organic-Inorganic Hybrids with Conjugated Polymers Based on POSS Having Heterogeneous Substituents. *Polymers* **2018**, *11*, 44.

(2) Liu, C.; Xiao, C.; Xie, C.; Li, W. Flexible Organic Solar Cells: Materials, Large-Area Fabrication Techniques and Potential Applications. *Nano Energy* **2021**, *89*, 106399.
(3) Corzo, D.; Tostado-Blázquez, G.; Baran, D. Flexible Electronics: Status, Challenges and Opportunities. *Front. Electron.* **2020**, *1*, 594003.
(4) Sharma, S.; Soni, R.; Kurungot, S.; Asha, S. K. Naphthalene Diimide Copolymers by Direct Arylation Polycondensation as Highly Stable Supercapacitor Electrode Materials. *Macromolecules* **2018**, *51*, 954−965.
(5) Sharma, S.; Kolhe, N. B.; Gupta, V.; Bharti, V.; Sharma, A.; Datt, R.; Chand, S.; Asha, S. K. Improved All-Polymer Solar Cell Performance of n-Type Naphthalene Diimide-Bithiophene P(NDI2OD-T2) Copolymer by Incorporation of Perylene Diimide as Coacceptor. *Macromolecules* **2016**, *49*, 8113−8125.
(6) Wavhal, B. A.; Ghosh, M.; Sharma, S.; Kurungot, S.; Sk, A. A High-Voltage Non-Aqueous Hybrid Supercapacitor Based on the N2200 Polymer Supported over Multiwalled Carbon Nanotubes. *Nanoscale* **2021**, *13*, 12314−12326.
(7) Sarang, K. T.; Miranda, A.; An, H.; Oh, E. S.; Verduzco, R.; Lutkenhaus, J. L. Poly(Fluorene- Alt-Naphthalene Diimide) as n-Type Polymer Electrodes for Energy Storage. *ACS Appl. Polym. Mater.* **2019**, *1*, 1155−1164.
(8) Ma, B.; Shi, Q.; Ma, X.; Li, Y.; Chen, H.; Wen, K.; Zhao, R.; Zhang, F.; Lin, Y.; Wang, Z.; Huang, H. Defect-Free Alternating Conjugated Polymers Enabled by Room- Temperature Stille Polymerization. *Angew. Chem., Int. Ed.* **2022**, *134*, No. e202115969.
(9) Pandey, M.; Kumari, N.; Nagamatsu, S.; Pandey, S. S. Recent Advances in the Orientation of Conjugated Polymers for Organic Field-Effect Transistors. *J. Mater. Chem. C* **2019**, *7*, 13323−13351.
(10) Carsten, B.; He, F.; Son, H. J.; Xu, T.; Yu, L. Stille Polycondensation for Synthesis of Functional Materials. *Chem. Rev.* **2011**, *111*, 1493−1528.
(11) Rudenko, A. E.; Wiley, C. A.; Tannaci, J. F.; Thompson, B. C. Optimization of Direct Arylation Polymerization Conditions for the Synthesis of Poly(3-Hexylthiophene). *J. Polym. Sci., Part A: Polym. Chem.* **2013**, *51*, 2660−2668.
(12) Hendsbee, A. D.; Li, Y. Performance Comparisons of Polymer Semiconductors Synthesized by Direct (Hetero)Arylation Polymerization (DHAP) and Conventional Methods for Organic Thin Film Transistors and Organic Photovoltaics. *Molecules* **2018**, *23*, 1255.
(13) Pouliot, J. R.; Grenier, F.; Blaskovits, J. T.; Beaupré, S.; Leclerc, M. Direct (Hetero)Arylation Polymerization: Simplicity for Conjugated Polymer Synthesis. *Chem. Rev.* **2016**, *116*, 14225−14274.
(14) Mercier, L. G.; Leclerc, M. Direct (Hetero)Arylation: A New Tool for Polymer Chemists. *Acc. Chem. Res.* **2013**, *46*, 1597−1605.
(15) Mainville, M.; Leclerc, M. Direct (Hetero)Arylation: A Tool for Low-Cost and Eco-Friendly Organic Photovoltaics. *ACS Appl. Polym. Mater.* **2021**, *3*, 2−13.
(16) Pirotte, G.; Agarkar, S.; Xu, B.; Zhang, J.; Lutsen, L.; Vanderzande, D.; Yan, H.; Pollet, P.; Reynolds, J. R.; Maes, W.; Marder, S. R. Molecular Weight Tuning of Low Bandgap Polymers by Continuous Flow Chemistry: Increasing the Applicability of PffBT4T for Organic Photovoltaics. *J. Mater. Chem. A* **2017**, *5*, 18166−18175.
(17) Yu, S.; Liu, F.; Yu, J.; Zhang, S.; Cabanetos, C.; Gao, Y.; Huang, W. Eco-Friendly Direct (Hetero)-Arylation Polymerization: Scope and Limitation. *J. Mater. Chem. C* **2017**, *5*, 29−40.
(18) Bura, T.; Blaskovits, J. T.; Leclerc, M. Direct (Hetero)Arylation Polymerization: Trends and Perspectives. *J. Am. Chem. Soc.* **2016**, *138*, 10056−10071.
(19) Grenier, F.; Goudreau, K.; Leclerc, M. Robust Direct (Hetero)Arylation Polymerization in Biphasic Conditions. *J. Am. Chem. Soc.* **2017**, *139*, 2816−2824.
(20) Marzano, G.; Carulli, F.; Babudri, F.; Pellegrino, A.; Po, R.; Luzzati, S.; Farinola, G. M. PBDTTPD for Plastic Solar Cells: Via Pd(PPh3)4-Catalyzed Direct (Hetero)Arylation Polymerization. *J. Mater. Chem. A* **2016**, *4*, 17163−17170.
(21) Pouliot, J. R.; Sun, B.; Leduc, M.; Najari, A.; Li, Y.; Leclerc, M. A High Mobility DPP-Based Polymer Obtained via Direct (Hetero)-Arylation Polymerization. *Polym. Chem.* **2015**, *6*, 278−282.
(22) Blaskovits, J. T.; Leclerc, M. C-H Activation as a Shortcut to Conjugated Polymer Synthesis. *Macromol. Rapid Commun.* **2019**, *40*, 1800512.
(23) Bura, T.; Beaupré, S.; Légaré, M. A.; Ibraikulov, O. A.; Leclerc, N.; Leclerc, M. Theoretical Calculations for Highly Selective Direct Heteroarylation Polymerization: New Nitrile-Substituted Dithienyl-Diketopyrrolopyrrole-Based Polymers. *Molecules* **2018**, *23*, 2324.
(24) Ye, L.; Schmitt, A.; Pankow, R. M.; Thompson, B. C. An Efficient Precatalyst Approach for the Synthesis of Thiazole-Containing Conjugated Polymers via Cu-Catalyzed Direct Arylation Polymerization (Cu-DArP). *ACS Macro Lett.* **2020**, *9*, 1446−1451.
(25) Dudnik, A. S.; Aldrich, T. J.; Eastham, N. D.; Chang, R. P. H.; Facchetti, A.; Marks, T. J. Tin-Free Direct C-H Arylation Polymerization for High Photovoltaic Efficiency Conjugated Copolymers. *J. Am. Chem. Soc.* **2016**, *138*, 15699−15709.
(26) Guo, C.; Quinn, J.; Sun, B.; Li, Y. Dramatically Different Charge Transport Properties of Bisthienyl Diketopyrrolopyrrole-Bithiazole Copolymers Synthesized: Via Two Direct (Hetero)-Arylation Polymerization Routes. *Polym. Chem.* **2016**, *7*, 4515−4524.
(27) Iizuka, E.; Wakioka, M.; Ozawa, F. Mixed-Ligand Approach to Palladium-Catalyzed Direct Arylation Polymerization: Synthesis of Donor-Acceptor Polymers with Dithienosilole (DTS) and Thienopyrroledione (TPD) Units. *Macromolecules* **2015**, *48*, 2989−2993.
(28) Kohn, P.; Huettner, S.; Steiner, U.; Sommer, M. Fractionated Crystallization of Defect-Free Poly(3-Hexylthiophene). *ACS Macro Lett.* **2012**, *1*, 1170−1175.
(29) Kakde, N. R.; Bharathkumar, H. J.; Wavhal, B. A.; Nikam, A.; Patil, S.; Dash, S. R.; Vanka, K.; Krishnamoorthy, K.; Kulkarni, A.; Asha, S. K. Direct (Hetero)Arylation (DHAP) Polymerization of Conjugated Polymers − New A−B−A Monomer Design for P(NDI2OD-T2) & the Challenges of Adopting DHAP for Continuous Flow Processes. *J. Mater. Chem. C* **2022**, *10*, 13025−13039.
(30) Kakde, N. R.; Asha, S. K. Exploring SiliaCat Pd-DPP as a Recyclable Heterogeneous Catalyst for the Multi-Batch Direct Heteroarylation Polymerization for P(NDI2OD-T2). *Polym. Chem.* **2023**, *14*, 2803−2819.
(31) Bura, T.; Morin, P. O.; Leclerc, M. En Route to Defect-Free Polythiophene Derivatives by Direct Heteroarylation Polymerization. *Macromolecules* **2015**, *48*, 5614−5620.
(32) Bura, T.; Beaupré, S.; Légaré, M. A.; Quinn, J.; Rochette, E.; Blaskovits, J. T.; Fontaine, F. G.; Pron, A.; Li, Y.; Leclerc, M. Direct Heteroarylation Polymerization: Guidelines for Defect-Free Conjugated Polymers. *Chem. Sci.* **2017**, *8*, 3913−3925.
(33) Gorelsky, S. I. Origins of Regioselectivity of the Palladium-Catalyzed (Aromatic)CH Bond Metalation-Deprotonation. *Coord. Chem. Rev.* **2013**, *257*, 153−164.
(34) Holycross, D. R.; Chai, M. Comprehensive NMR Studies of the Structures and Properties of PEI Polymers. *Macromolecules* **2013**, *46*, 6891−6897.
(35) Hussaini, S. R.; Kuta, A.; Pal, A.; Wang, Z.; Eastman, M. A.; Duran, R. Application of NMR Spectroscopy for the Detection of Equilibrating E- Z Diastereomers. *ACS Omega* **2020**, *5*, 24848−24853.
(36) René, O.; Fagnou, K. Room-Temperature Direct Arylation of Polyfluorinated Arenes under Biphasic Conditions. *Org. Lett.* **2010**, *12*, 2116−2119.
(37) Nikam, S. B.; Pratap, C.; Krishnamurty, S.; Asha, S. K. Structure-Property Insights into Chiral Thiophene Copolymers by Direct Heteroarylation Polymerization. *Eur. Polym. J.* **2022**, *181*, 111676.
(38) Matsidik, R.; Komber, H.; Luzio, A.; Caironi, M.; Sommer, M. Defect-Free Naphthalene Diimide Bithiophene Copolymers with Controlled Molar Mass and High Performance via Direct Arylation Polycondensation. *J. Am. Chem. Soc.* **2015**, *137*, 6705−6711.

https://doi.org/10.1021/acspolymersau.4c00050
ACS Polym. Au 2024, 4, 449−459

(39) Zhao, K.; Zhang, T.; Zhang, L.; Li, J.; Li, H.; Wu, F.; Chen, Y.; Zhang, Q.; Han, Y. Role of Molecular Weight in Microstructural Transition and Its Correlation to the Mechanical and Electrical Properties of P(NDI2OD-T2) Thin Films. *Macromolecules* **2021**, *54*, 10203−10215.

(40) Kakde, N. R. *Green Approaches for Synthesis and Scale-up of π-Conjugated Polymers (Enrollment Number 10CC17J26038)*; Acedmy of Scientific and Innovative ResearchCenter, 2023 https://1drv.ms/b/c/c85a5898b7e79079/Ef9qUGmZPeBKiQfyAgnoOuwBbG2CaQHpQ6bS8x4XrQ0Itgand NationalChemicalLaboratoryPune.

https://doi.org/10.1021/acspolymersau.4c00050
ACS Polym. Au 2024, 4, 449−459